

Fusion hindrance of heavy ions: Role of the neck

David Boilley* and Hongliang Lü

GANIL, CEA/DSM-CNRS/IN2P3, BP 55027, F-14076 Caen cedex 5, France and Université de Caen Basse-Normandie, BP 5186, F-14032 Caen Cedex, France

Caiwan Shen

School of Science, Huzhou Teachers College, Huzhou, 313000 Zhejiang, People's Republic of China

Yasuhisa Abe

Research Center for Nuclear Physics, Osaka University, 10-1 Mihogaoka, Ibaraki, 567-0047 Osaka, Japan

Bertrand G. Giraud

Institut Physique Théorique, CEA/DSM, Centre d'Etudes-Saclay, Gif-sur-Yvette, F-91191, France

(Received 28 July 2011; published 7 November 2011)

Fusion of heavy ions is largely hindered because of the appearance of an inner barrier between the contact point of the two colliding nuclei and the compound nucleus. But there are still quantitative ambiguities on the size of the barrier and on the role of the dissipation. In this paper we stress the importance of the neck of the composite system on the hindrance of the fusion of heavy nuclei. We show that the “denecking” process is very quick compared to the other collective degrees of freedom as the relative distance. This behavior of the neck will change the potential seen by the relative distance on the way to fusion and its effective initial value through a dynamical coupling. Both effects contribute to the hindrance of fusion.

DOI: [10.1103/PhysRevC.84.054608](https://doi.org/10.1103/PhysRevC.84.054608)

PACS number(s): 25.70.Jj, 24.10.Pa

I. INTRODUCTION

Fusion of heavy ions is largely hindered by comparison to what is observed for lighter systems. This has been observed experimentally for many years [1,2] and is nowadays qualitatively understood: After crossing the Coulomb barrier, the fusing system at contact must overcome a second barrier under strong dissipation. This inner barrier does not exist for lighter systems that directly reach the compound state after crossing the Coulomb barrier. Such an interpretation is commonly accepted [3–16], but there are still quantitative ambiguities on the dynamics of the fusion mechanism and predictions might not be reliable.

Experimentally, it is very difficult to distinguish between the fusion-fission events that have reached the compound state and the quasifission ones that reparate after crossing the Coulomb barrier. This leads to a lack of reliable data on fusion cross sections that could assess the models. The assessment of the various models used to describe the complete fusion process is then one of the main challenges of the field. For a recent review, see, e.g., Ref. [17].

Theoretically, the fusion process is divided into two steps corresponding to the crossing of the two consecutive barriers [8]. For the Coulomb barrier, an extrapolation of the simple models used for lighter systems without hindrance is sometime used [15,18,19] and we can rely on the experimental capture cross sections. Actually, the dissipation process cannot be neglected during this step for heavy ions because of the large Coulomb field. It leads to a partial explanation of the

fusion hindrance [20,21]. Coupled-channels codes can nicely reproduce experimental data for light systems, even far below the barrier. But the inclusion of some dissipation mechanisms that would be necessary for energies over the barrier is still under development [22–24].

The main contribution to the fusion hindrance observed in heavy ions is due to the second step, consisting of a diffusion process over an inner potential barrier. The main features of the dynamics of this so-called formation phase are well understood: Most of the models are based on stochastic equations [6–16]. This is justified by the fact that the intrinsic degrees of freedom had enough time to thermalize during the crossing of the Coulomb barrier. But ambiguities remain on the size of the barrier and the strength of the dissipation.

Another difficulty arises from the fact that the two steps of the fusion process cannot be treated with a single formalism. We have to deal with a parametrization for the two-body system crossing the Coulomb barrier and with another one for the composite from the contact point to the compound shape. The treatment of the connection between the two descriptions is a delicate problem that can change the final results.

As we will show in this article, the fusion process is very sensitive to the treatment of the evolution of the neck between the two colliding nuclei at contact, because the size of the barrier that has to be overcome strongly depends on it (see Fig. 1). The formation probability depends exponentially on this barrier and, depending on the treatment, the final fusion cross section can differ by orders of magnitude. It is important to note that some of the previous studies on the effect of the neck on the fusion process are related to the Coulomb barrier [25,26]. Here, we focus our work on the inner barrier.

*boilley@ganil.fr

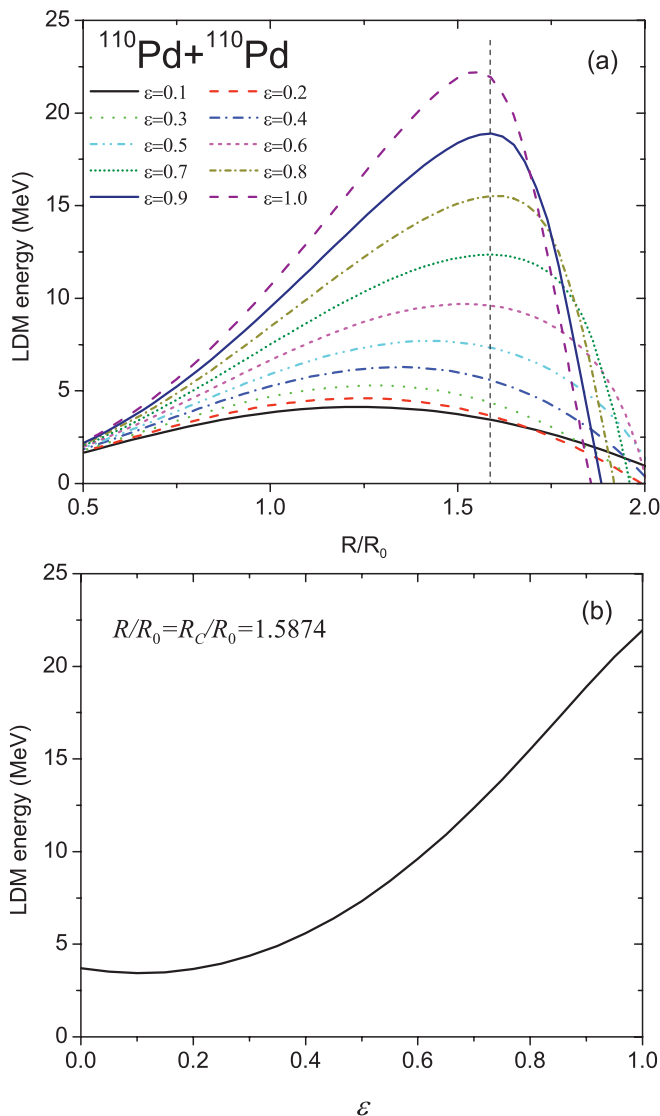


FIG. 1. (Color online) (Top) Liquid drop model potential energy of the system $^{110}\text{Pd}+^{110}\text{Pd}$ as a function of the elongation coordinate for various neck parameters. ϵ is the neck parameter and R_0 the radius of the compound nucleus. The vertical dashed line on the top panel represents the contact position. (Bottom) Liquid drop model potential energy as a function of the neck parameter along the contact line.

In some studies, the neck was supposed to be frozen at a given value that was arbitrarily fixed [13,14] or adjusted to fit some experimental fusion cross sections [8]. References [27,28] claim that the previous hypothesis is correct: A dynamical study suggests that the neck does not evolve much during the fusion process. In some other works [10–12], the inner potential barriers are evaluated by minimization with respect to the neck. The “denecking” process, i.e., the disappearance of the cleft between the two nuclei at contact, is also very fast in the fusion trajectory chosen in Refs. [29,30] to calculate the potential barriers. In preliminary versions of this work reported in Refs. [31–34] and in Refs. [35,36], it is shown on dynamical arguments that it is correct. Finally, in Refs. [15,16] the neck degree of freedom is not mentioned.

The previous models are based on macroscopic approaches. There are also theories to describe the fusion process with microscopic models based on mean-field theory or molecular dynamics. But there are very few connections between microscopic and macroscopic approaches. In Ref. [21], macroscopic parameters were extracted from a mean-field approach, but this study is limited to the Coulomb barrier. To our knowledge, Ref. [35] is a rare study of the dynamics of the neck studied from a microscopic approach based on molecular dynamics.

How is the neck evolving during the fusion process? What is the most suitable value of this variable? What does it mean for the other collective variables? We have to answer to these questions in order to understand the fusion mechanism.

II. SIMPLIFIED NECK DYNAMICS

The neck parameter ϵ is related to the cleft between the two touching nuclei. $\epsilon = 1$ corresponds to two hard touching spheres and $\epsilon = 0$ to the absence of cleft. More precisely, in our calculations, the neck parameter is taken from the two-center parametrization [37] and is defined by the potential shape of the interacting nuclei. The dissipation is calculated with the wall-and-window formalism [38,39].

The dynamics of the formation phase is frequently based on coupled stochastic equations [6–16]. The other two variables are the relative distance between the centers of mass of the two nuclei and the mass asymmetry of the colliding system. These collective degrees of freedom are connected through the liquid drop model (LDM) potential, the collective inertia and friction. But as a first step, we will study the dynamics of the neck separately.

As for the LDM potential, it turns out that it is almost linear in the neck parameter at contact (see Fig. 1). Then, for a simple analysis of the neck dynamics, we solve analytically the Smoluchowski equation with a linear potential,

$$\frac{\partial N(\epsilon, t)}{\partial t} = C \frac{\partial N(\epsilon, t)}{\partial \epsilon} + D \frac{\partial^2 N(\epsilon, t)}{\partial \epsilon^2}, \quad (1)$$

where $C = f/\gamma$ and the diffusion coefficient $D = kT/\gamma$. Here f is a constant parameter such as $V(\epsilon) = f\epsilon$ and γ is the friction coefficient. Since the neck parameter is limited to the $[0, 1]$ interval, we will add two reflective boundaries in $\epsilon = 0$ and $\epsilon = 1$.

With a single reflective boundary in $\epsilon = 0$ and an initial distribution taken as $N_1(\epsilon, 0) = \delta(\epsilon - \epsilon_0)$, the Smoluchowski equation (1) was solved in Refs. [40–42],

$$N_1(\epsilon, t) = \frac{1}{\sqrt{4\pi Dt}} \exp\left[-\frac{C}{2D}(\epsilon - \epsilon_0) - \frac{C^2 t}{4D}\right] \times \left\{ \exp\left[-\frac{(\epsilon - \epsilon_0)^2}{4Dt}\right] + \exp\left[-\frac{(\epsilon + \epsilon_0)^2}{4Dt}\right] \right\} + \frac{C}{2D} \exp\left(-\frac{C\epsilon}{D}\right) \text{erfc}\left(\frac{\epsilon + \epsilon_0 - Ct}{2\sqrt{Dt}}\right). \quad (2)$$

For large times, this expression becomes a Boltzmann distribution. The average value of the neck was calculated

in Ref. [43],

$$\begin{aligned} \langle \varepsilon(t) \rangle = & \varepsilon_0 - Ct + \frac{1}{2} \left(\frac{D}{C} - \varepsilon_0 + Ct \right) \operatorname{erfc} \left(\frac{\varepsilon_0 - Ct}{\sqrt{4Dt}} \right) \\ & - \frac{D}{2C} \exp \left(\frac{C\varepsilon_0}{D} \right) \operatorname{erfc} \left(\frac{\varepsilon_0 + Ct}{\sqrt{4Dt}} \right) \\ & + \sqrt{\frac{Dt}{\pi}} \exp \left[-\frac{(\varepsilon_0 - Ct)^2}{4Dt} \right]. \end{aligned} \quad (3)$$

We also solved the problem with the two reflective boundaries, following the method of Refs. [41,44] and get,

$$\begin{aligned} N_2(\varepsilon, t) = & \frac{C}{D} \frac{\exp(-\frac{C\varepsilon}{D})}{1 - \exp(-\frac{Ca}{D})} \\ & + \exp \left[-\frac{C}{2D}(\varepsilon - \varepsilon_0) - \frac{C^2 t}{4D} \right] \\ & \times \sum_{k=1}^{\infty} \left\{ \exp \left(-\frac{k^2 \pi^2 D}{a^2} t \right) \frac{2}{a \left(1 + \frac{C^2 a^2}{4D^2 k^2 \pi^2} \right)} \right. \\ & \times \left[\cos \left(\frac{k\pi\varepsilon}{a} \right) - \frac{C}{2D} \frac{a}{k\pi} \sin \left(\frac{k\pi\varepsilon}{a} \right) \right] \\ & \times \left. \left[\cos \left(\frac{k\pi\varepsilon_0}{a} \right) - \frac{C}{2D} \frac{a}{k\pi} \sin \left(\frac{k\pi\varepsilon_0}{a} \right) \right] \right\}. \end{aligned} \quad (4)$$

For the sake of generality, we denote the position of the second reflective boundary by a . The average value of the neck as a function of time can be obtained in a similar way,

$$\begin{aligned} \langle \varepsilon(t) \rangle = & \frac{D}{C} + \frac{a}{1 - \exp(-\frac{Ca}{D})} \\ & + 32a\pi^2 D^4 \exp \left(\frac{C}{2D}\varepsilon_0 - \frac{C^2 t}{4D} \right) \\ & \times \sum_{k=1}^{\infty} \left\{ \exp \left(-\frac{k^2 \pi^2 D}{a^2} t \right) \frac{k^2}{(a^2 C^2 + 4D^2 k^2 \pi^2)^2} \right. \\ & \times \left[\cos \left(\frac{k\pi\varepsilon_0}{a} \right) - \frac{C}{2D} \frac{a}{k\pi} \sin \left(\frac{k\pi\varepsilon_0}{a} \right) \right] \\ & \times \left. \left[(-1)^k \exp \left(-\frac{Ca}{2D} \right) - 1 \right] \right\}. \end{aligned} \quad (5)$$

In Fig. 2, we plot the neck distribution and its average value as a function of time for the two cases. With such a strong slope of the potential, the reflecting wall in a does not play any role. If we arbitrarily decrease this slope, the curves corresponding to the two situations differ in a clear manner.

It appears that the neck evolves very quickly to its asymptotic distribution for both cases. For small times, the average value of the neck is approximately

$$\langle \varepsilon(t) \rangle \simeq \varepsilon_0 - Ct. \quad (6)$$

There is an ambiguity on the initial value of the neck parameter since the denecking process might already start before crossing the Coulomb barrier [25,26]. With the extreme hypothesis that the initial neck parameter is close to 1, the time scale to reach small values for the neck parameter is then of the order of $1/C = \gamma/f$. Typical values of C are ranging from 1.1 to 2.7 MeV/ \hbar .

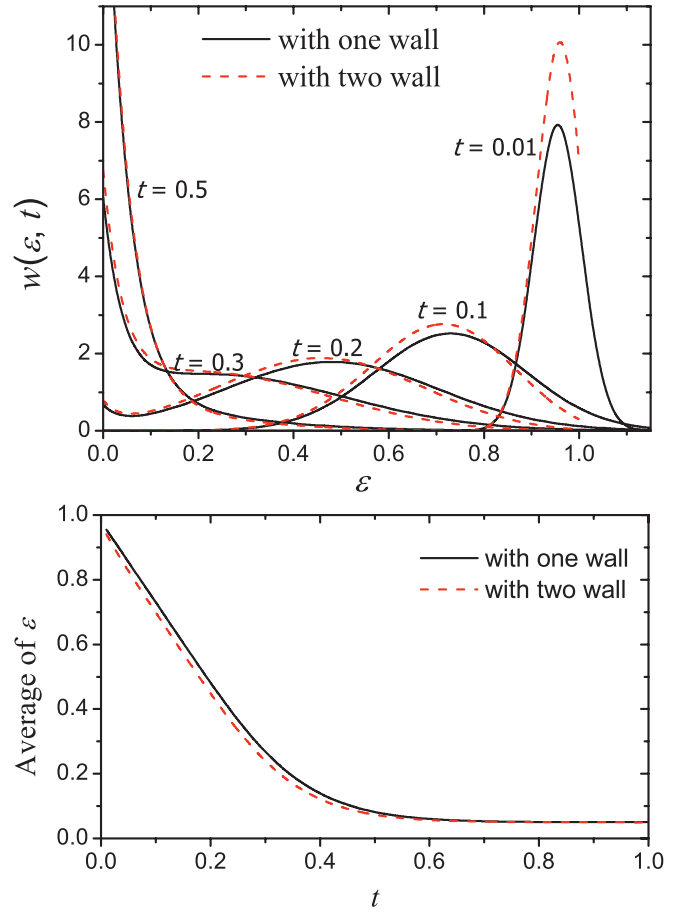


FIG. 2. (Color online) Neck distribution and its average value as a function of time. The solid line corresponds to the case with one reflecting wall in $\varepsilon = 0$ and the dashed one to the case with two reflective walls, in $\varepsilon = 0$ and 1. Here $C = 2.5$ MeV/ \hbar and $D = 0.125$ MeV/ \hbar , which are typical values. Time is indicated in \hbar/MeV . Here, the initial value of the neck is arbitrarily chosen as $\varepsilon_0 = 0.95$.

The time scale of the fusion process along the relative distance was evaluated with a similar approach in Ref. [45]. For a diffusive process corresponding to the actual situation, the typical time to overcome the potential barrier is about one order of magnitude longer. Then, the time scale of the evolution of the neck is far shorter than the radial one and we can, as a first approximation, consider that the neck is completely thermalized during the second stage of the fusion process.

Actually, the potential shown in Fig. 1 is not linear for small values of ε . Unfortunately, analytical solutions are not available for higher order potentials with reflective boundaries. But, the linear approximation is valid for the initial values of the neck. A dynamical study with a more realistic potential will not change the characteristic time for the neck to reach small values. It will only affect the final thermal distribution.

Reference [35] shows the time evolution of the neck calculated with a microscopic model and it appears that it is also shorter than the time characterizing the evolution of the relative distance. The velocity is peaked as function of time and vanishes on a time scale of the order of 100 fm/c or 0.5 \hbar/MeV , which is similar to our result. Our conclusion

differs from the one of Refs. [27,28] that claim that the neck is frozen around a value of about 0.7, but is in agreement with the hypothesis done in Refs. [10–12,29,30].

Our analysis gives a quantitative confirmation of the discussion of Ref. [12]: the neck degree of freedom is quickly drifted by a strong potential slope, which is due to the large surface energy gain of the denecking process. With typical values of the potential for heavy nuclei, the thermalized neck parameter is very small, around or lower than 0.1.

III. APPEARANCE OF THE HINDRANCE

The size and the location of the inner barrier along the relative distance that is calculated with the LDM are very sensitive to the neck (see Fig. 1). Depending on the relative position of this barrier to the contact point of the two colliding nuclei, the fusion will be hindered or not. Then, the

experimental appearance of the hindrance should give some constraints on the location of the inner barrier and then the size of the neck [9,33].

For symmetric reactions, the large hindrance phenomenon appears somewhere between the $^{100}\text{Mo}+^{100}\text{Mo}$ and the $^{110}\text{Pd}+^{110}\text{Pd}$ systems [2]. Then the overlap of the inner barrier and the contact point should occur between these two systems if one considers the contact point as the injection point of the formation process. For the $^{100}\text{Mo}+^{100}\text{Mo}$ system, the LDM potential landscape calculated within the two-center parametrization [37] is plotted in Fig. 3. It can be seen that the contact point is beyond this barrier, whatever the neck parameter. Then, after contact, the composite system is driven to the compound shape without hindrance. The situation differs for the $^{110}\text{Pd}+^{110}\text{Pd}$ system, see Figs. 1 and 3. For small values of the neck ε , there is a large barrier between the contact point and the compound shape. For larger values of ε , the contact position is closer to the edge of the potential map. Then the neck parameter has to be smaller than 0.6 to explain the large hindrance of the fusion that is experimentally observed.

Although data are missing on symmetric systems between $^{100}\text{Mo}+^{100}\text{Mo}$ and $^{110}\text{Pd}+^{110}\text{Pd}$ to have a more precise analysis, this simple argument is in favor of our claim that the neck parameter should be small when the system crosses the inner barrier. The analysis presented here is limited to symmetric reactions. We did a systematic analysis of the border between hindered and nonhindered reactions that confirm the fact that the neck should disappear quickly [9,46].

IV. COUPLING OF THE NECK TO THE OTHER DEGREES OF FREEDOM

We are now convinced that the denecking process occurs very quickly compared to the typical time scale of the other degrees of freedom determining the fusion. The main argument is based on the potential landscape: the dynamics of the relative distance between the centers of mass of the two nuclei is governed by the diffusion over a potential barrier, which is a slow process [45], whereas the neck is driven by a strong potential slope toward its asymptotic value. But these collective variables are also coupled dynamically through the inertia and friction tensors.

Here, for the sake of simplicity, we only consider two degrees of freedom: the relative distance between the two centers R and the neck ε . This will limit our analysis to symmetric reactions. The formation dynamics can be described by the two-dimension Langevin equation

$$\gamma \begin{bmatrix} \dot{\varepsilon} \\ \dot{r} \end{bmatrix} = - \begin{bmatrix} \partial V / \partial \varepsilon \\ \partial V / \partial r \end{bmatrix} + \begin{bmatrix} \rho_1(t) \\ \rho_2(t) \end{bmatrix}, \quad (7)$$

for which we have neglected the inertia term, in order to be consistent with the Smoluchowski approximation. The random force satisfies the fluctuation-dissipation theorem,

$$\langle \rho_i(t) \rho_j(t') \rangle = 2T \gamma_{ij} \delta(t - t'). \quad (8)$$

In this equation, r is a dimensionless variable defined as $r = R/R_0$, R_0 being the radius of the compound nucleus.

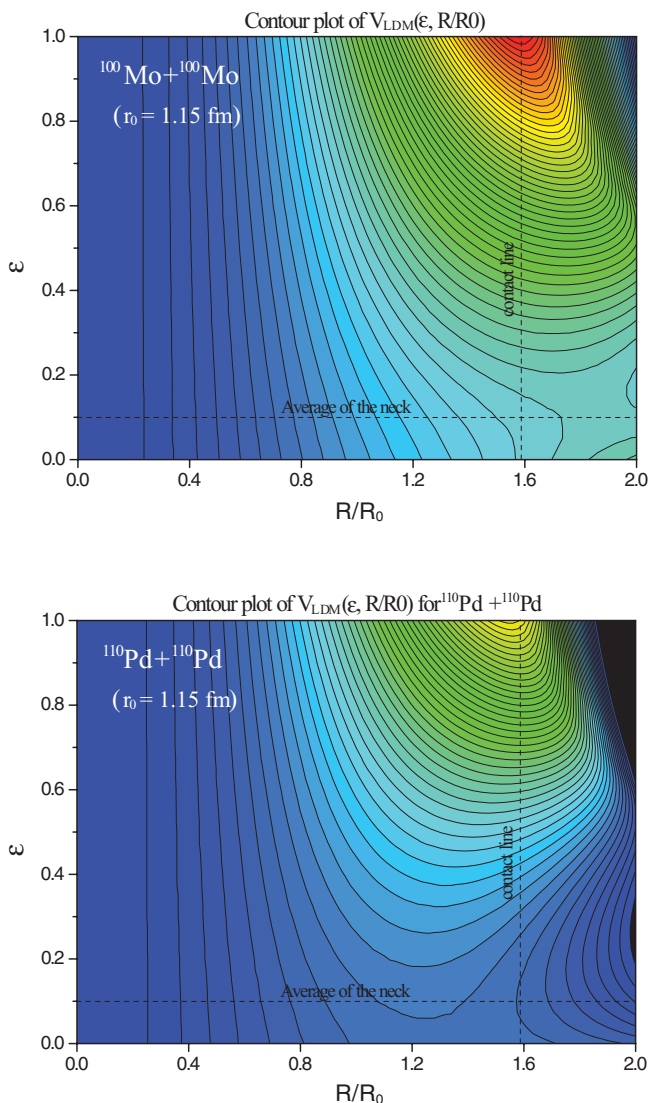


FIG. 3. (Color online) LDM potential map for $^{100}\text{Mo}+^{100}\text{Mo}$ (top) and $^{110}\text{Pd}+^{110}\text{Pd}$ (bottom) as a function of the relative distance and neck parameter.

We will assume here that around the saddle, the friction tensor γ is independent of r and ε . The potential map is such as it has a U shape for the neck variable and a barrier shape for the radial one. Then, the fast neck dynamics could be approximately studied as follow,

$$\dot{\varepsilon} = -[\gamma^{-1}]_{\varepsilon\varepsilon} \frac{\partial V}{\partial \varepsilon} - [\gamma^{-1}]_{r\varepsilon} \frac{\partial V}{\partial r} + r_\varepsilon(t) \quad (9)$$

$$\simeq -[\gamma^{-1}]_{\varepsilon\varepsilon} \frac{\partial V}{\partial \varepsilon} - [\gamma^{-1}]_{r\varepsilon} \frac{\partial V}{\partial r} \Big|_{r=r_0} + r_\varepsilon(t). \quad (10)$$

We will assume further that r_0 is close to the saddle point and $|\frac{\partial V}{\partial \varepsilon}|_{\varepsilon=\varepsilon_0} \gg |\frac{\partial V}{\partial r}|_{r=r_0}$. Then, we can neglect the second term of the right-hand side of Eq. (10),

$$\dot{\varepsilon} \simeq -[\gamma^{-1}]_{\varepsilon\varepsilon} \frac{\partial V}{\partial \varepsilon} + r_\varepsilon(t). \quad (11)$$

Once the neck has reached its asymptotic value, the large confinement potential confines the neck variable.

The differential equation governing the evolution of r ,

$$\gamma_{r\varepsilon} \dot{\varepsilon} + \gamma_{rr} \dot{r} = -\frac{\partial V}{\partial r} + \rho_2(t), \quad (12)$$

should be studied on two time scales: first, during the quick evolution of the neck variable, the average value can be approximated by

$$\gamma_{r\varepsilon} \langle \dot{\varepsilon} \rangle + \gamma_{rr} \langle \dot{r} \rangle \simeq 0, \quad (13)$$

which means that

$$\Delta \langle r \rangle \simeq -\frac{\gamma_{r\varepsilon}}{\gamma_{rr}} \Delta \langle \varepsilon \rangle. \quad (14)$$

Here, we have also neglected the term $\frac{\partial V}{\partial r}$ because during this transient regime $\frac{\partial V}{\partial \varepsilon}$ is dominating. The initial variance of the relative distance is also related to the final variance of the neck variable corresponding to the Boltzmann distribution:

$$\langle \delta r^2(0) \rangle = \frac{\gamma_{r\varepsilon}^2}{\gamma_{rr}^2} \langle \delta \varepsilon^2(\infty) \rangle. \quad (15)$$

Once the neck is confined, i.e., $\dot{\varepsilon} \simeq 0$, one then has

$$\gamma_{rr} \dot{r} \simeq -\frac{\partial V}{\partial r} + \rho_2(t), \quad (16)$$

which is a simple one-dimensional Langevin equation for the relative distance only, with an initial condition that is shifted according to Eqs. (14) and (15).

This approximate dynamical evolution can be checked on a simple test case based on a harmonic potential that is not meant to be realistic,

$$V(\varepsilon, r) = V_s + \frac{1}{2} g \varepsilon^2 - \frac{1}{2} h (r - r_s)^2, \quad (17)$$

for which the coupled differential Eqs. (7) can be exactly solved [47]. With such a potential, the approximate evolution of r is characterized by

$$\langle r(t) - r_s \rangle = \left[(r_0 - r_s) + \frac{\gamma_{r\varepsilon}}{\gamma_{rr}} (\varepsilon_0 - \varepsilon_\infty) \right] \exp\left(\frac{ht}{\gamma_{rr}}\right) \quad (18)$$

and

$$\langle \delta r^2(t) \rangle = \frac{T}{h} \left[\exp\left(\frac{2ht}{\gamma_{rr}}\right) - 1 \right] + \langle \delta r^2(0) \rangle \exp\left(\frac{2ht}{\gamma_{rr}}\right). \quad (19)$$

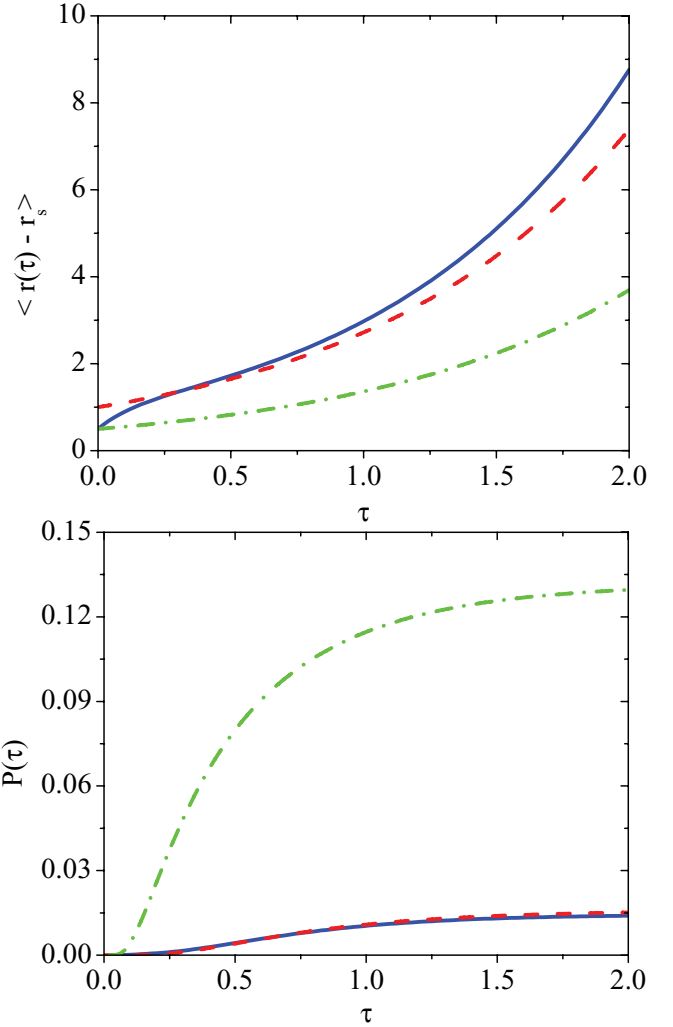


FIG. 4. (Color online) Average trajectory (top) and fusion probability (down) as a function of time for a parabolic potential. The solid blue line represents the exact solution. The green dotted-dashed one represents the uncoupled one ($\gamma_{r\varepsilon} = 0$). The dashed red curve represents the approximate solution (see text). Here $\gamma_{\varepsilon\varepsilon}/\gamma_{rr} = 0.6$, $\gamma_{r\varepsilon}/\gamma_{rr} = 0.5$, $g/h = 3$, and $T/h = 0.2$. The time unit is γ_{rr}/h .

Figure 4 shows the comparison of this result with the exact solution given in the appendix and the uncoupled case ($\gamma_{r\varepsilon} = 0$) for the average trajectory and the fusion probability,

$$P(t) = \int_{-\infty}^{r_s} \exp\left[-\frac{(r - \langle r(t) \rangle)^2}{2\delta r^2(t)}\right] \frac{dr}{\sqrt{2\pi\delta r^2(t)}} \quad (20)$$

$$= \frac{1}{2} \operatorname{erfc}\left[\frac{\langle r(t) - r_s \rangle}{\sqrt{2\delta r^2(t)}}\right]. \quad (21)$$

Here we took $\varepsilon_\infty = 0$ as given by the Boltzmann distribution. The approximate solution of Eqs. (18), (19), and (21) agrees quite nicely with the exact solution, although $g/h = 3$ is quite weak. For larger values of g/h , the accuracy is even better. Note that this simple model and its approximation are valid only near the saddle.

It appears clearly that the fast evolution of the neck variable allows us to study the evolution of the other degrees of freedom

separately. In the previous sections, we showed that the potential map is very sensitive to the value of the neck. Here, we find that the dynamical coupling through the dissipation tensor shifts the effective initial value of the relative distance [see Eq. (14)].

Initially, the neck is far from its equilibrium value. Its large and fast variation shifts the effective initial value of the relative distance. After this transient regime, the fusion will then follow the path that minimizes the potential with respect to the neck and we can do an adiabatic approximation.

With this simple model, the shift is of the order of few femtometers, which is large enough to have an influence on the hindrance of the fusion. It explains the large difference between the fusion probabilities of the uncoupled case and the approximate or exact coupled case that can be observed on Fig. 4. The shift of the initial value of the relative distance is always positive in this model and enlarges the size of the barrier that has to be crossed to reach the compound shape. The fusion is then more hindered.

The effect of the shift of the effective injection point on the long time limit of the fusion probability,

$$P(t \rightarrow \infty) = \frac{1}{2} \operatorname{erfc} \left[\sqrt{\frac{V(\varepsilon_\infty, r_s) - V(\varepsilon_\infty, r_0 - r_s + \Delta r)}{T}} \right], \quad (22)$$

is the larger the heavier the system. For systems close to the hindrance border, such as $^{110}\text{Pd}+^{110}\text{Pd}$, r_0 is close to the saddle and the potential is quite flat. For heavier systems, the potential has a steeper slope near the contact point. Therefore, the shift Δr will cause a larger change of the potential barrier for heavier systems.

Of course, the model here is crude: the potential landscape is simple, we neglected the inertia, and we assumed that the friction tensor is constant. It confirms the adiabatic approximation that is usually done in the various models, but it shows that the dynamical coupling between the neck and radial degrees of freedom induces a shift of the effective initial value of the relative distance. We will publish another article with a more comprehensive study on its magnitude.

Actually, in their so-called fusion by diffusion model, Świątecki *et al.* [12] introduced an initial shift of the injection point considered to be an adjustable parameter ranging from 0 to 3 fm. Here, we propose a justification to it. More recently, Liu *et al.* [48] explore numerically the effect of the nondiagonal term of the friction tensor on the injection point. They conclude that the average injection point is not shifted. This contradicts our results.

V. CONCLUSION

Since superheavy elements are produced in extremely small numbers, their main characteristics are not yet accessible. But, using a fission-evaporation code, it is possible to constrain strongly the shell-correction energy of their ground state [33,49] if we know the fusion probability. Unfortunately, experimental fusion cross sections are not reliable because it is very difficult to distinguish between fission and quasifission. Fusion models should then be assessed by other means.

In this article, we have stressed the importance of the neck parameter that can change the fusion cross sections by orders of magnitude. We have shown that the neck degree of freedom evolves faster than the relative distance between the two fusing nuclei. Then the approximation of using an asymptotic value of the neck is justified.

The rapid evolution of the neck parameter changes the potential landscape seen by the other collective variables. The experimental appearance of the hindrance of the fusion for symmetric reactions confirms this conclusion. This rapid evolution of the neck also changes the initial value of the other collective variables through a dynamical coupling. For the relative distance, the shift is not negligible and should be included in the models. Our analysis gives a theoretical justification to the adjustable shift introduced by Świątecki *et al.* [12] in order to reproduce the data. Finally, it is important to note that both effects enlarge the hindrance of the fusion.

This analysis of the influence of the neck dynamics on the fusion of heavy nuclei is mainly based on simplified analytical models and is, therefore, limited to symmetric reactions. The asymmetry degree of freedom complicates the analysis which cannot be simply handled with analytical toy models. Therefore, a more complete study will be published in another article.

ACKNOWLEDGMENTS

We are indebted to Y. Lallouet for helpful remarks. The present work was supported by the JSPS Grant Nos. 18540268 and L10708, by the Natural Science Foundation of China under Grant Nos. 10979024 and 10905021, the Key project of Science and Technology Research of Ministry of Education of China under Grant No. 209053, and the Natural Science Foundation of Zhejiang province, China under Grant No. Y6090210 and by the LIA GANIL-RIKEN. The authors also acknowledge support and hospitality by RCNP Osaka University, GANIL, Huzhou Teachers College, and IPT, CE-Saclay, which enabled us to continue the collaboration.

APPENDIX : EXACT SOLUTION OF THE DIFFUSION OVER THE PARABOLIC POTENTIAL

Following the method of Ref. [47], it is possible to solve exactly the diffusion problem in the overdamped limit on the potential landscape of Eq. (17). The distributions are Gaussian characterized by

$$\langle \varepsilon(t) \rangle = \varepsilon_0 \frac{e^{a+t} + e^{a-t}}{2} + \frac{e^{a-t} - e^{a+t}}{2\sqrt{\Delta}} \times [2(r_0 - r_s)\gamma_{r\varepsilon}h + \varepsilon_0(\gamma_{\varepsilon\varepsilon}h + \gamma_{rr}g)] \quad (A1)$$

$$\langle \delta\varepsilon^2(t) \rangle = \frac{T\gamma_{rr}}{\gamma_{rr}\gamma_{\varepsilon\varepsilon} - \gamma_{r\varepsilon}^2} \left\{ \frac{e^{2a+t} - 1}{2a_+\sqrt{\Delta}} \left(\sqrt{\Delta} + 2\frac{h\gamma_{r\varepsilon}^2}{\gamma_{rr}} - \gamma_{\varepsilon\varepsilon}h - \gamma_{rr}g \right) + \frac{e^{2a-t} - 1}{2a_-\sqrt{\Delta}} \times \left(\sqrt{\Delta} - 2\frac{h\gamma_{r\varepsilon}^2}{\gamma_{rr}} + \gamma_{\varepsilon\varepsilon}h + \gamma_{rr}g \right) \right\}, \quad (A2)$$

with

$$a_{\pm} = \frac{\gamma_{\varepsilon\varepsilon}h - \gamma_{rr}g \pm \sqrt{\Delta}}{2(\gamma_{rr}\gamma_{\varepsilon\varepsilon} - \gamma_{r\varepsilon}^2)} \quad (\text{A3})$$

$$\Delta = (\gamma_{\varepsilon\varepsilon}h - \gamma_{rr}g)^2 + 4gh(\gamma_{rr}\gamma_{\varepsilon\varepsilon} - \gamma_{r\varepsilon}^2). \quad (\text{A4})$$

Here the friction tensor is symmetric: $\gamma_{r\varepsilon} = \gamma_{\varepsilon r}$. Without off-diagonal term ($\gamma_{r\varepsilon} = 0$), these expressions simply become

$$\langle \varepsilon(t) \rangle = \varepsilon_0 e^{-\frac{gt}{\gamma_{\varepsilon\varepsilon}}} \quad (\text{A5})$$

$$\langle \delta\varepsilon^2(t) \rangle = \frac{T}{g} (1 - e^{-2\frac{gt}{\gamma_{\varepsilon\varepsilon}}}). \quad (\text{A6})$$

With the approximation of Eq. (10), we have

$$\langle \varepsilon(t) \rangle \simeq -\frac{\gamma_{r\varepsilon}h}{\gamma_{rr}g} (r_0 - r_s) (1 - e^{-g[\gamma^{-1}]_{\varepsilon\varepsilon}t}) + \varepsilon_0 e^{-g[\gamma^{-1}]_{\varepsilon\varepsilon}t} \quad (\text{A7})$$

$$\langle \delta\varepsilon^2(t) \rangle \simeq \frac{T}{g} (1 - e^{-2g[\gamma^{-1}]_{\varepsilon\varepsilon}t}). \quad (\text{A8})$$

For long times, we then take the average value given by the Boltzmann distribution as an asymptotic value of the neck variable, $\langle \varepsilon(t \rightarrow \infty) \rangle = \varepsilon_{\infty}$.

Similarly, for r , the exact solution is characterized by

$$\langle r(t) \rangle = r_s + (r_0 - r_s) \frac{e^{a_+t} + e^{a_-t}}{2} + [2\varepsilon_0\gamma_{r\varepsilon}g + (r_0 - r_s)(\gamma_{\varepsilon\varepsilon}h + \gamma_{rr}g)] \frac{e^{a_+t} - e^{a_-t}}{2\sqrt{\Delta}} \quad (\text{A9})$$

$$\langle \delta r^2(t) \rangle = \frac{T\gamma_{\varepsilon\varepsilon}}{\gamma_{rr}\gamma_{\varepsilon\varepsilon} - \gamma_{r\varepsilon}^2} \left\{ \frac{e^{2a_+t} - 1}{2a_+\sqrt{\Delta}} \left(\sqrt{\Delta} - 2\frac{g\gamma_{r\varepsilon}^2}{\gamma_{\varepsilon\varepsilon}} + \gamma_{\varepsilon\varepsilon}h + \gamma_{rr}g \right) + \frac{e^{2a_-t} - 1}{2a_-\sqrt{\Delta}} \times \left(\sqrt{\Delta} + 2\frac{g\gamma_{r\varepsilon}^2}{\gamma_{\varepsilon\varepsilon}} - \gamma_{\varepsilon\varepsilon}h - \gamma_{rr}g \right) \right\}. \quad (\text{A10})$$

When the two variables are uncoupled ($\gamma_{r\varepsilon} = 0$), these expressions simply become

$$\langle r(t) \rangle = r_s + (r_0 - r_s) e^{\frac{ht}{\gamma_{rr}}} \quad (\text{A11})$$

$$\langle \delta r^2(t) \rangle = \frac{T}{h} (e^{2\frac{ht}{\gamma_{rr}}} - 1). \quad (\text{A12})$$

The approximate solution is characterized by Eqs. (18) and (19).

-
- [1] C.-C. Sahn, H.-G. Clerc, K.-H. Schmidt, W. Reisdorf, P. Armbruster, F. P. Heßberger, J. G. Keller, G. Münzenberg, and D. Vermeulen, *Z. Phys. A* **319**, 113 (1984).
- [2] K.-H. Schmidt and W. Morawek, *Rep. Prog. Phys.* **54**, 949 (1991).
- [3] W. J. Świątecki, *Nucl. Phys. A* **376**, 275 (1982).
- [4] G. Royer and B. Remaud, *Nucl. Phys. A* **444**, 477 (1985).
- [5] J. P. Blocki, H. Feldmeier and W. J. Świątecki, *Nucl. Phys. A* **459**, 145 (1986).
- [6] Y. Abe, D. Boilley, G. Kosenko, J. D. Bao, C. W. Shen, B. G. Giraud, and T. Wada, *Prog. Theor. Phys. Suppl.* **146**, 104 (2002).
- [7] Y. Abe, C. W. Shen, G. I. Kosenko, and D. Boilley, *Phys. At. Nucl.* **66**, 1057 (2003).
- [8] C. Shen, G. Kosenko, and Y. Abe, *Phys. Rev. C* **66**, 061602(R) (2002).
- [9] C. Shen, Y. Abe, Q. Li, and D. Boilley, *Sci. China G* **52**, 1458 (2009).
- [10] W. J. Świątecki, K. Siwek-Wilczyńska, and J. Wilczyński, *Acta Phys. Pol. B* **34**, 2049 (2003).
- [11] W. J. Świątecki, K. Siwek-Wilczyńska, and J. Wilczyński, *Int. J. Mod. Phys. E* **13**, 261 (2004).
- [12] W. J. Świątecki, K. Siwek-Wilczyńska, and J. Wilczyński, *Phys. Rev. C* **71**, 014602 (2005).
- [13] Y. Aritomo and M. Ohta, *Nucl. Phys. A* **744**, 3 (2004).
- [14] Y. Aritomo, *Nucl. Phys. A* **780**, 222 (2006).
- [15] V. I. Zagrebaev, *Phys. Rev. C* **64**, 034606 (2001).
- [16] V. Zagrebaev and W. Greiner, *J. Phys. G* **31**, 825 (2005).
- [17] D. Hinde, R. du Rietz, and M. Dasgupta, *EPJ Web of Conferences* **17**, 04001 (2011).
- [18] K. Siwek-Wilczyńska, E. Siemaszko, and J. Wilczyński, *Acta Phys. Pol. B* **33**, 451 (2002).
- [19] K. Siwek-Wilczyńska and J. Wilczyński, *Phys. Rev. C* **69**, 024611 (2004).
- [20] N. Rowley, N. Grar, and K. Hagino, *Phys. Lett. B* **632**, 243 (2006).
- [21] K. Washiyama, D. Lacroix, and S. Ayik, *Phys. Rev. C* **79**, 024609 (2009).
- [22] C. M. Ko, *Z. Phys. A* **286**, 405 (1978).
- [23] A. Diaz-Torres, D. J. Hinde, M. Dasgupta, G. J. Milburn, and J. A. Tostevin, *Phys. Rev. C* **78**, 064604 (2008).
- [24] S. Yusa, K. Hagino, and N. Rowley, *Phys. Rev. C* **82**, 024606 (2010).
- [25] C. E. Aguiar, V. C. Barbosa, L. F. Canto, and R. Donangelo, *Nucl. Phys. A* **472**, 571 (1987).
- [26] A. Iwamoto and K. Harada, *Z. Phys. A* **326**, 201 (1987).
- [27] J. D. Bao, *Int. J. Mod. Phys. E* **15**, 1625 (2006).
- [28] G. G. Adamian, N. V. Antonenko, A. Diaz-Torres, and W. Scheid, *Nucl. Phys. A* **671**, 233 (2000).
- [29] R. Moustabchir and G. Royer, *Nucl. Phys. A* **683**, 266 (2001).
- [30] G. Royer, K. Zbiri, and C. Bonilla, *Nucl. Phys. A* **730**, 355 (2004).
- [31] Y. Abe, C. W. Shen, G. Kosenko, D. Boilley, and B. Giraud, *Int. J. Mod. Phys. E* **17**, 2214 (2008).
- [32] Y. Abe, C. W. Shen, D. Boilley, and B. Giraud, *Int. J. Mod. Phys. E* **18**, 2169 (2009).
- [33] D. Boilley, Y. Abe, C. W. Shen and B. Yilmaz, CERN-Proceedings-2010-001, 479 (2010).
- [34] D. Boilley, C. Shen, Y. Abe, and B. G. Giraud, *EPJ Web of Conferences* **17**, 10001 (2011).
- [35] K. Zhao, Z. Li, X. Wu, and Z. Zhao, *Phys. Rev. C* **79**, 024614 (2009).
- [36] Z.-H. Liu and J.-D. Bao, *Phys. Rev. C* **81**, 044606 (2010).
- [37] K. Sato, A. Iwamoto, K. Harada, S. Yamaji, and S. Yoshida, *Z. Phys. A* **288**, 383 (1978).
- [38] J. Blocki, Y. Boneh, J. R. Nix, J. Randrup, M. Robel, A. J. Sierk, and W. J. Świątecki, *Ann. Phys.* **113**, 330 (1978).
- [39] T. Wada, Y. Abe, and N. Carjan, *Phys. Rev. Lett.* **70**, 3538 (1993).
- [40] M. v. Smoluchowski, *Phys. Z.* **17**, 585 (1916).
- [41] M. Mason and W. Weaver, *Phys. Rev.* **23**, 412 (1924).
- [42] S. Chandrasekar, *Rev. Mod. Phys.* **15**, 1 (1943).

- [43] B. U. Felderhof, *J. Stat. Phys.* **109**, 483 (2002).
- [44] H. Minowa and N. Mishima, *Lett. Nuovo Cimento* **37**, 99 (1983).
- [45] D. Boilley, Y. Abe, and J. D. Bao, *Eur. Phys. J. A* **18**, 627 (2003).
- [46] C. Shen, D. Boilley, Q. Li, J. Shen, and Y. Abe, *Phys. Rev. C* **83**, 054620 (2011).
- [47] Y. Abe, D. Boilley, B. G. Giraud, and T. Wada, *Phys. Rev. E* **61**, 1125 (2000).
- [48] Zu-Hua Liu and Jing-Dong Bao, *Phys. Rev. C* **83**, 044613 (2011).
- [49] A. Marchix, Ph.D. thesis, Université de Caen, 2007.